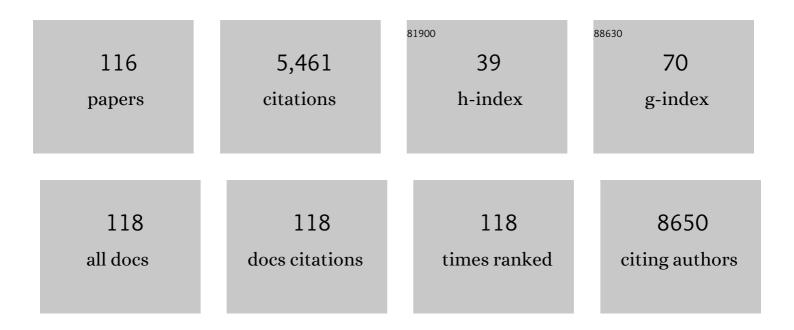
Lia A Stanciu

List of Publications by Year in descending order

Source: https://exaly.com/author-pdf/506684/publications.pdf Version: 2024-02-01



Ι ΙΑ Δ STANCIU

#	Article	IF	CITATIONS
1	Fabrication of High-Surface-Area Graphene/Polyaniline Nanocomposites and Their Application in Supercapacitors. ACS Applied Materials & Interfaces, 2013, 5, 2685-2691.	8.0	309
2	Nanohybrids of a MXene and transition metal dichalcogenide for selective detection of volatile organic compounds. Nature Communications, 2020, 11, 1302.	12.8	294
3	Surface Functionalization of Ti ₃ C ₂ T _{<i>x</i>} MXene with Highly Reliable Superhydrophobic Protection for Volatile Organic Compounds Sensing. ACS Nano, 2020, 14, 11490-11501.	14.6	247
4	Graphene-modified nanostructured vanadium pentoxide hybrids with extraordinary electrochemical performance for Li-ion batteries. Nature Communications, 2015, 6, 6127.	12.8	201
5	Structure of TRPV1 channel revealed by electron cryomicroscopy. Proceedings of the National Academy of Sciences of the United States of America, 2008, 105, 7451-7455.	7.1	194
6	Understanding Pt Nanoparticle Anchoring on Graphene Supports through Surface Functionalization. ACS Catalysis, 2016, 6, 2642-2653.	11.2	172
7	Covalently-grafted polyaniline on graphene oxide sheets for high performance electrochemical supercapacitors. Carbon, 2014, 71, 257-267.	10.3	171
8	Effect of temperature and moisture on the miscibility of amorphous dispersions of felodipine and poly(vinyl pyrrolidone). Journal of Pharmaceutical Sciences, 2010, 99, 169-185.	3.3	169
9	Natural Biopolymers: Novel Templates for the Synthesis of Nanostructures. Langmuir, 2010, 26, 8497-8502.	3.5	167
10	Enzyme functionalized nanoparticles for electrochemical biosensors: A comparative study with applications for the detection of bisphenol A. Biosensors and Bioelectronics, 2010, 26, 43-49.	10.1	123
11	Novel Pyrolyzed Polyaniline-Grafted Silicon Nanoparticles Encapsulated in Graphene Sheets As Li-Ion Battery Anodes. ACS Applied Materials & Interfaces, 2014, 6, 5996-6002.	8.0	114
12	Graphene based enzymatic bioelectrodes and biofuel cells. Nanoscale, 2015, 7, 6909-6923.	5.6	113
13	Aptamer-based SERS biosensor for whole cell analytical detection of E.Âcoli O157:H7. Analytica Chimica Acta, 2019, 1081, 146-156.	5.4	92
14	Sulfur-Doped Titanium Carbide MXenes for Room-Temperature Gas Sensing. ACS Sensors, 2020, 5, 2915-2924.	7.8	92
15	Investigation of the Interaction between Nafion Ionomer and Surface Functionalized Carbon Black Using Both Ultrasmall Angle X-ray Scattering and Cryo-TEM. ACS Applied Materials & Interfaces, 2017, 9, 6530-6538.	8.0	89
16	Microfluidic rapid and autonomous analytical device (microRAAD) to detect HIV from whole blood samples. Lab on A Chip, 2019, 19, 3375-3386.	6.0	86
17	Graphene-titanium dioxide nanocomposite based hypoxanthine sensor for assessment of meat freshness. Biosensors and Bioelectronics, 2017, 89, 518-524.	10.1	82
18	Surface Functionalization of Layered Molybdenum Disulfide for the Selective Detection of Volatile Organic Compounds at Room Temperature. ACS Applied Materials & Interfaces, 2019, 11, 34135-34143.	8.0	79

#	Article	IF	CITATIONS
19	AChE biosensor based on zinc oxide sol–gel for the detection of pesticides. Analytica Chimica Acta, 2010, 661, 195-199.	5.4	78
20	Competitive heavy metal adsorption onto new and aged polyethylene under various drinking water conditions. Journal of Hazardous Materials, 2020, 385, 121585.	12.4	77
21	An aqueous media based approach for the preparation of a biosensor platform composed of graphene oxide and Pt-black. Biosensors and Bioelectronics, 2012, 38, 314-320.	10.1	74
22	Effects of impaired membrane interactions on α-synuclein aggregation and neurotoxicity. Neurobiology of Disease, 2015, 79, 150-163.	4.4	73
23	Reusable photocatalytic titanium dioxide–cellulose nanofiber films. Journal of Colloid and Interface Science, 2013, 399, 92-98.	9.4	70
24	Magnetic Particle-Based Hybrid Platforms for Bioanalytical Sensors. Sensors, 2009, 9, 2976-2999.	3.8	69
25	Bisphenol A detection using gold nanostars in a SERS improved lateral flow immunochromatographic assay. Sensors and Actuators B: Chemical, 2018, 276, 222-229.	7.8	63
26	Investigation of a Catalyst Ink Dispersion Using Both Ultra-Small-Angle X-ray Scattering and Cryogenic TEM. Langmuir, 2010, 26, 19199-19208.	3.5	62
27	Cu2O and Au/Cu2O Particles: Surface Properties and Applications in Glucose Sensing. Sensors, 2012, 12, 13019-13033.	3.8	61
28	Preparation of high-surface-area carbon nanoparticle/graphene composites. Carbon, 2012, 50, 3845-3853.	10.3	57
29	Overexpression of alpha-synuclein at non-toxic levels increases dopaminergic cell death induced by copper exposure via modulation of protein degradation pathways. Neurobiology of Disease, 2015, 81, 76-92.	4.4	57
30	Core/shell nanoparticles as hybrid platforms for the fabrication of a hydrogen peroxide biosensor. Journal of Materials Chemistry, 2010, 20, 5030.	6.7	56
31	Aminolated and Thiolated PECâ€Covered Gold Nanoparticles with High Stability and Antiaggregation for Lateral Flow Detection of Bisphenol A. Small, 2018, 14, 1702828.	10.0	56
32	Functionalized graphene oxide for the fabrication of paraoxon biosensors. Analytica Chimica Acta, 2014, 827, 86-94.	5.4	51
33	Multifunctional calcium carbonate microparticles: Synthesis and biological applications. Journal of Materials Chemistry, 2010, 20, 7728.	6.7	50
34	Hierarchical polybenzimidazole-grafted graphene hybrids as supports for Pt nanoparticle catalysts with excellent PEMFC performance. Nano Energy, 2015, 16, 281-292.	16.0	50
35	Au nanospheres and nanorods for enzyme-free electrochemical biosensor applications. Biosensors and Bioelectronics, 2011, 26, 4514-4519.	10.1	49
36	Microfluidic paper-based aptasensor devices for multiplexed detection of pathogenic bacteria. Biosensors and Bioelectronics, 2022, 207, 114214.	10.1	49

#	Article	IF	CITATIONS
37	Biomagnetic Glasses: Preparation, Characterization, and Biosensor Applications. Langmuir, 2010, 26, 4320-4326.	3.5	46
38	Hierarchical Nanocomposites of Vanadium Oxide Thin Film Anchored on Graphene as High-Performance Cathodes in Li-Ion Batteries. ACS Applied Materials & Interfaces, 2014, 6, 18894-18900.	8.0	46
39	Impedimetric Dengue Biosensor based on Functionalized Graphene Oxide Wrapped Silica Particles. Electrochimica Acta, 2016, 194, 422-430.	5.2	46
40	Recent Advances in Aptamer-Based Biosensors for Global Health Applications. Annual Review of Biomedical Engineering, 2021, 23, 433-459.	12.3	41
41	Fe3O4–SiO2 nanocomposites obtained via alkoxide and colloidal route. Journal of Sol-Gel Science and Technology, 2006, 40, 317-323.	2.4	40
42	CeO2–MO x (M: Zr, Ti, Cu) mixed metal oxides with enhanced oxygen storage capacity. Journal of Materials Science, 2015, 50, 3750-3762.	3.7	40
43	Novel CeO2–CuO-decorated enzymatic lactate biosensors operating in low oxygen environments. Analytica Chimica Acta, 2016, 909, 121-128.	5.4	39
44	Bimetallic PdCu/SPCE non-enzymatic hydrogen peroxide sensors. Sensors and Actuators B: Chemical, 2015, 220, 968-976.	7.8	38
45	Self-assembly and alignment of semiconductor nanoparticles on cellulose nanocrystals. Journal of Materials Science, 2011, 46, 5672-5679.	3.7	37
46	Mechanical properties and corrosion behavior of powder metallurgy iron-hydroxyapatite composites for biodegradable implant applications. Materials and Design, 2016, 109, 556-569.	7.0	37
47	Hybrid plasmonic Au–TiN vertically aligned nanocomposites: a nanoscale platform towards tunable optical sensing. Nanoscale Advances, 2019, 1, 1045-1054.	4.6	37
48	Facile Preparation of Graphene/SnO ₂ Xerogel Hybrids as the Anode Material in Li-Ion Batteries. ACS Applied Materials & Interfaces, 2015, 7, 27087-27095.	8.0	36
49	Cold drawn bioabsorbable ferrous and ferrous composite wires: An evaluation of in vitro vascular cytocompatibility. Acta Biomaterialia, 2013, 9, 8574-8584.	8.3	35
50	InÂVitro Study of α-Synuclein Protofibrils by Cryo-EM Suggests aÂCu2+-Dependent Aggregation Pathway. Biophysical Journal, 2013, 104, 2706-2713.	0.5	35
51	Microarc oxidation discharge types and bio properties of the coating synthesized on zirconium. Materials Science and Engineering C, 2017, 77, 374-383.	7.3	35
52	Inkjet Printed Nanopatterned Aptamerâ€Based Sensors for Improved Optical Detection of Foodborne Pathogens. Small, 2019, 15, e1805342.	10.0	35
53	Spark Plasma Sintering of ZrB2–SiC–ZrC ultra-high temperature ceramics at 1800°C. Materials Science & Engineering A: Structural Materials: Properties, Microstructure and Processing, 2011, 528, 6079-6082.	5.6	34
54	Bioresorbable Fe–Mn and Fe–Mn–HA Materials for Orthopedic Implantation: Enhancing Degradation through Porosity Control. Advanced Healthcare Materials, 2017, 6, 1700120.	7.6	33

#	Article	IF	CITATIONS
55	Investigation of porosity on mechanical properties, degradation and in-vitro cytotoxicity limit of Fe30Mn using space holder technique. Materials Science and Engineering C, 2019, 99, 1048-1057.	7.3	31
56	Influence of powder precursors on reaction sintering of Al2TiO5. Scripta Materialia, 2004, 50, 1259-1262.	5.2	30
57	Evolution of novel bioresorbable iron-manganese implant surfaces and their degradation behaviors in vitro. Journal of Biomedical Materials Research - Part A, 2015, 103, 185-193.	4.0	30
58	A Sensitive Electrochemical H ₂ O ₂ Sensor Based on PdAg-Decorated Reduced Graphene Oxide Nanocomposites. Journal of the Electrochemical Society, 2016, 163, B379-B384.	2.9	30
59	Layer by layer construction of ascorbate interference-free amperometric lactate biosensors with lactate oxidase, ascorbate oxidase, and ceria nanoparticles. Mikrochimica Acta, 2016, 183, 1667-1675.	5.0	30
60	Inkjet printed electrochemical aptasensor for detection of Hg2+ in organic solvents. Electrochimica Acta, 2019, 316, 33-42.	5.2	30
61	Direct fabrication of crystalline hydroxyapatite coating on zirconium by single-step plasma electrolytic oxidation process. Surface and Coatings Technology, 2016, 301, 74-79.	4.8	29
62	In Vivo Evaluation of Biodegradability and Biocompatibility of Fe30Mn Alloy. Veterinary and Comparative Orthopaedics and Traumatology, 2018, 31, 010-016.	0.5	29
63	Optical Biosensors for Diagnostics of Infectious Viral Disease: A Recent Update. Diagnostics, 2021, 11, 2083.	2.6	29
64	Field-assisted sintering of Li1.3Al0.3Ti1.7(PO4)3 solid-state electrolyte. Solid State Ionics, 2015, 278, 217-221.	2.7	27
65	Cold-Drawn Bioabsorbable Ferrous and Ferrous Composite Wires: An Evaluation of Mechanical Strength and Fatigue Durability. Metallurgical and Materials Transactions B: Process Metallurgy and Materials Processing Science, 2012, 43, 984-994.	2.1	26
66	DNA-Functionalized Ti ₃ C ₂ T <i>_x</i> MXenes for Selective and Rapid Detection of SARS-CoV-2 Nucleocapsid Gene. ACS Applied Nano Materials, 2022, 5, 1902-1910.	5.0	26
67	Protein-templated semiconductor nanoparticle chains. Nanotechnology, 2008, 19, 275602.	2.6	24
68	The effect of heating rate and composition on the properties of spark plasma sintered zirconium diboride based composites. Materials Science & Engineering A: Structural Materials: Properties, Microstructure and Processing, 2012, 538, 98-102.	5.6	24
69	Effects of microstructure and heat treatment on mechanical properties and corrosion behavior of powder metallurgy derived Fe–30Mn alloy. Materials Science & Engineering A: Structural Materials: Properties, Microstructure and Processing, 2017, 703, 214-226.	5.6	24
70	Roll-to-Roll Manufactured Sensors for Nitroaromatic Organophosphorus Pesticides Detection. ACS Applied Materials & Interfaces, 2021, 13, 35961-35971.	8.0	24
71	Polybenzimidazole (PBI) Functionalized Nanographene as Highly Stable Catalyst Support for Polymer Electrolyte Membrane Fuel Cells (PEMFCs). Journal of the Electrochemical Society, 2016, 163, F1228-F1236.	2.9	20
72	Origin of High Interfacial Resistances in Solid‣tate Batteries: Interdiffusion and Amorphous Film Formation in Li 0.33 La 0.57 TiO 3 /LiMn 2 O 4 Half Cells. ChemElectroChem, 2019, 6, 4576-4585.	3.4	20

#	Article	IF	CITATIONS
73	Electricâ€Field Effects on Sintering and Reaction to Form Aluminum Titanate from Binary Alumina–Titania Sol–Gel Powders. Journal of the American Ceramic Society, 2001, 84, 983-985.	3.8	19
74	Effect of microstructure and strain on the degradation behavior of novel bioresorbable iron–manganese alloy implants. Journal of Biomedical Materials Research - Part A, 2015, 103, 738-745.	4.0	19
75	Nanoporous metals for biodegradable implants: Initial bone mesenchymal stem cell adhesion and degradation behavior. Journal of Biomedical Materials Research - Part A, 2016, 104, 1747-1758.	4.0	19
76	Surface modifications through dealloying of Fe–Mn and Fe–Mn–Zn alloys developed to create tailorable, nanoporous, bioresorbable surfaces. Acta Materialia, 2016, 103, 115-127.	7.9	19
77	Cold decorated polystyrene particles for lateral flow immunodetection of Escherichia coli O157:H7. Mikrochimica Acta, 2017, 184, 4879-4886.	5.0	19
78	Simultaneous colorimetric and electrochemical detection of trace mercury (Hg2+) using a portable and miniaturized aptasensor. Biosensors and Bioelectronics, 2023, 221, 114419.	10.1	19
79	Initial Stages of Sintering of Alumina by Thermo-Optical Measurements. Journal of the American Ceramic Society, 2007, 90, 2716-2722.	3.8	18
80	Synthesis of CeO2-based core/shell nanoparticles with high oxygen storage capacity. International Nano Letters, 2017, 7, 187-193.	5.0	18
81	Selective Detection of Ethylene by MoS ₂ –Carbon Nanotube Networks Coated with Cu(l)–Pincer Complexes. ACS Sensors, 2020, 5, 1699-1706.	7.8	18
82	Fabrication of ZnS nanoparticle chains on a protein template. Journal of Nanoparticle Research, 2009, 11, 2031-2041.	1.9	14
83	Ionic Strength Influences on Biofunctional Au-Decorated Microparticles for Enhanced Performance in Multiplexed Colorimetric Sensors. ACS Applied Materials & Interfaces, 2020, 12, 32397-32409.	8.0	14
84	Structural Evolution During Reaction to Form Aluminum Titanate from Sol-Gel Precursors. Materials and Manufacturing Processes, 2004, 19, 641-650.	4.7	13
85	Collagen Coating Effects on Fe–Mn Bioresorbable Alloys. Journal of Orthopaedic Research, 2020, 38, 523-535.	2.3	12
86	Versatile printed microheaters to enable low-power thermal control in paper diagnostics. Analyst, The, 2020, 145, 184-196.	3.5	12
87	An <i>in vitro</i> model for preclinical testing of thrombogenicity of resorbable metallic stents. Journal of Biomedical Materials Research - Part A, 2015, 103, 2118-2125.	4.0	11
88	Reactive Hot Pressing and Properties of Zr _{1â^'<i>x</i>} Ti _{<i>x</i>} B ₂ –ZrC Composites. Journal of the American Ceramic Society, 2015, 98, 711-716.	3.8	11
89	Improving bioactivity of inert bioceramics by a novel Mg-incorporated solution treatment. Applied Surface Science, 2017, 425, 564-575.	6.1	10
90	Application of corn zein as an anchoring molecule in a carbon nanotube enhanced electrochemical sensor for the detection of gliadin. Food Control, 2020, 117, 107350.	5.5	10

#	ARTICLE	IF	CITATIONS
91	In Situ Synthesis and Characterization of Zr-Based Amorphous Composite by Laser Direct Deposition. Metallurgical and Materials Transactions A: Physical Metallurgy and Materials Science, 2015, 46, 4316-4325.	2.2	9
92	Preparation and characterization of alumina supported silicalite membranes by sol–gel hydrothermal method. Journal of Membrane Science, 2002, 210, 197-207.	8.2	8
93	Biotemplated Silica and Titania Nanowires: Synthesis, Characterization and Potential Applications. Journal of Nanoscience and Nanotechnology, 2012, 12, 227-235.	0.9	8
94	Cu(II) promotes amyloid pore formation. Biochemical and Biophysical Research Communications, 2015, 464, 342-347.	2.1	8
95	An in-vitro study: The effect of surface properties on bioactivity of the oxide layer fabricated on Zr substrate by PEO. Surfaces and Interfaces, 2021, 22, 100884.	3.0	8
96	Origin of High Interfacial Resistance in Solidâ€State Batteries: LLTO/LCO Half ells**. ChemElectroChem, 2021, 8, 1847-1857.	3.4	8
97	Title is missing!. Journal of Sol-Gel Science and Technology, 2000, 19, 839-843.	2.4	7
98	Electrochemical Biosensors Fabricated with Polyelectrolyte Microspheres. Journal of the Electrochemical Society, 2012, 159, B783-B788.	2.9	7
99	Antidelaminating, Thermally Stable, and Cost-Effective Flexible Kapton Platforms for Nitrate Sensors, Mercury Aptasensors, Protein Sensors, and p-Type Organic Thin-Film Transistors. ACS Applied Materials & Interfaces, 2021, 13, 11369-11384.	8.0	7
100	ZrB ₂ ‧iC and ZrB ₂ â€ZrC Ceramics with High Secondary Phase Content. International Journal of Applied Ceramic Technology, 2015, 12, E44.	2.1	6
101	Two C-terminal sequence variations determine differential neurotoxicity between human and mouse α-synuclein. Molecular Neurodegeneration, 2020, 15, 49.	10.8	6
102	Investigation of the Interaction of Nafion Ionomer and Carbon Black Using Small Angle X-ray and Small Angle Neutron Scattering. ECS Transactions, 2011, 41, 637-645.	0.5	5
103	Nisin infusion into surface cracks in oxide coatings to create an antibacterial metallic surface. Materials Science and Engineering C, 2019, 105, 110034.	7.3	5
104	Folding dynamics of phenylalanine hydroxylase depends on the enzyme's metallation state: the native metal, iron, protects against aggregate intermediates. European Biophysics Journal, 2011, 40, 959-968.	2.2	4
105	Tuning a Bisphenol A Lateral Flow Assay Using Multiple Gold Nanosystems. Particle and Particle Systems Characterization, 2019, 36, 1900133.	2.3	4
106	Interphases Formation and Analysis at the Lithium–Aluminum–Titanium–Phosphate (LATP) and Lithium–Manganese Oxide Spinel (LMO) Interface during Highâ€Temperature Bonding. Energy Technology, 2020, 8, 2000634.	3.8	4
107	Investigation of Catalyst Ink Dispersion Using Small Angle X-ray and Small Angle Neutron Scattering. ECS Transactions, 2010, 33, 1335-1345.	0.5	2
108	Nanostructured Graphenes and Metal Oxides for Fuel Cell and Battery Applications. Advanced Materials Research, 0, 705, 126-131.	0.3	2

#	Article	IF	CITATIONS
109	Biodegradable materials for medical applications. , 2022, , 307-346.		2
110	Inkjet Printing platforms for DNA-based pathogen detection. NIP & Digital Fabrication Conference, 2018, 34, 107-112.	0.0	2
111	Effect of High Heating Rates on Microstructure of Alumina and Aluminum Titanate Ceramics. Microscopy and Microanalysis, 2001, 7, 414-415.	0.4	1
112	Preparation of biomolecule gel matrices for electron microscopy. Ultramicroscopy, 2008, 108, 309-313.	1.9	1
113	Structural Evolution During Reaction to Form Aluminum Titanate from Sol-Gel Precursors. Materials and Manufacturing Processes, 2004, 19, 641-650.	4.7	1
114	Bioâ€Nanopatterning: Inkjet Printed Nanopatterned Aptamerâ€Based Sensors for Improved Optical Detection of Foodborne Pathogens (Small 24/2019). Small, 2019, 15, 1970128.	10.0	0
115	Composite biomaterials. , 2022, , 149-169.		Ο
116	Materials and devices for sensors and detectors. , 2022, , 267-306.		0